Band gap engineering by functionalization of BN sheet

A. Bhattacharya, S. Bhattacharya, and G. P. Das*

Department of Materials Science, Indian Association for the Cultivation of Science, Jadavpur, Kolkata 700032, India

(Received 17 May 2011; revised manuscript received 8 December 2011; published 9 January 2012)

From first principles calculations, we investigate the stability and physical properties of single-layer *h*-BN sheet chemically functionalized by various groups, viz. H, F, OH, CH_3, CHO, CN, NH_2, etc. We find that full functionalization of *h*-BN sheet with these groups leads to decrease in its electronic band gap, albeit to different magnitudes varying from 0.3 eV to 3.1 eV, depending upon the dopant group. Functionalization by a CHO group in particular leads to a sharp decrease in the electronic band gap of the pristine BN sheet to ∼0.3 eV, which is congenial for its usage in transistor-based devices. For the optimized structure of the sheet, the calculated phonon frequencies corresponding to all the vibrational modes turn out to be real (positive), thereby suggesting their inherent stability. The chemisorption energies of these groups with the B and N atoms of the sheet are found to lie in the range of 1.5–6 eV. The optical absorption and conductivity of these functionalized sheets under polarized light are found to be much higher than that of the native BN sheet.

DOI: 10.1103/PhysRevB.85.035415 PACS number(s): 71.20.−b, 63.22.Np, 71.15.Mb, 62.23.Kn

I. INTRODUCTION

Graphene,[1] the two-dimensional (2D) sp^2-bonded single layer of graphite, is in great demand today because of its unique combination of electrical[2] and mechanical[3] properties. Because the conductivity of graphene is very high (its electrons act as massless fermions), its usage in electronic devices can be made possible only if one can somehow introduce a band gap (close to those of conventional semiconductors such as Si, GaAs) in it. In the past, various methods have been implemented for engineering the band gap of planar nanostructures.[4–6] Chemical modification of graphene by functionalizing its surface with various dopants provides one such avenue for opening of a band gap and has been found to be useful in band gap engineering of graphene.[7] In fact, the fully hydrogenated derivative of graphene, known as graphane,[8–10] has been experimentally synthesized in the laboratory[11] and is found to have an insulating band gap of ∼3.5 eV. Another analogous 2D nanostructure, viz. hexagonal boron nitride sheet (*h*-BN sheet),[12] has emerged as a strong candidate in this field because of its similar hexagonal planar geometry to graphene, combined with diverse (or contrasting) electronic properties. *h*-BN sheet has been experimentally synthesized in single and multiple layers.[13,14] While graphene is a semimetal with unique 2D conducting properties, *h*-BN is a typical insulator. Hydrogenation of a *h*-BN sheet leads to reduction in the band gap of the sheet, opposite to the trend observed in the case of graphene.[15] Thus, chemical modification seems to be a natural tool for tuning the gap in both the graphene and BN sheet. In both the graphene and BN sheet, H passivation takes place in such a way that one H atom gets bonded to each of the C or B and N atoms of the sheet in specific periodic fashion, giving rise to various possible structural conformers of the sheet, viz. chair, boat, and stirrup.[8–10,15] In the chair and boat conformers, the H atom alternates singly and in pair on both sides of the sheet,[8–10,15] while in the stirrup conformer, three consecutive H atoms alternate on either side of the sheet.[10,15] In graphane, the chair conformer has been found to have the highest stability.[8–10] However, in the case of the hydrogenated *h*-BN sheet, the stirrup conformer is found to have the highest stability [binding energy (BE) of ∼4.84 eV/atom],[15] followed by boat and chair conformers. Though chemical modification of graphene has been studied and experimented by several groups, the same in a *h*-BN sheet has not been explored exhaustively until this date.

In this paper we estimate from our first principles-based calculations the stability and ground-state properties of the *h*-BN sheet chemically functionalized by various groups, viz. H, F, OH, CH_3, CHO, CN, NH_2, etc. Using these dopants, the band gaps of these chemically modified sheets can be tuned from 3.1 eV to 0.3 eV. The phonon calculations play an important role in determining the inherent stability of these sheets. Therefore, we have also plotted the phonon dispersion and density of states (DOS) to show that the frequencies corresponding to all the vibrational modes in these sheets are real (positive), thereby suggesting their inherent stability. We have also plotted the optical absorption spectra of these functionalized BN sheets under light polarized perpendicular to the BN plane. The optical absorption and the conductivity in these functionalized sheets are found to be much higher than those of the native BN sheets.

II. COMPUTATIONAL DETAILS

First-principles density functional theory (DFT)[16,17] based on total energy calculations has been carried out using VASP[18] code with projected augmented wave (PAW) potential[19] for all elemental constituents of these functionalized sheets. The calculations have been performed using the Ceperley-Alder (CA) exchange-correlation functional[20] within the local density approximation (LDA). We have also compared the LDA band gap results with generalized gradient approximation (GGA) using PW-91 exchange correlation.[21] An energy cut off of 600 eV has been used. The k-mesh was generated by a Monkhorst-Pack[22] method, and the results were tested for convergence with respect to mesh size [8 × 8 × 4]. However, for the generation of the DOS and band-structure plots, higher values of k-points [16 × 16 × 8] were used. In all our calculations, self-consistency has been achieved with a 0.0001 eV convergence in total energy. For optimizing the ground-state geometry,[23,24] atomic forces were converged to less than 0.001 eV/Å via conjugate gradient minimization. The

 ©2012 American Physical Society

phonon dispersion has been computed using the variational density functional perturbation theory (DFPT),[25] while the optical calculations are performed by using DFT within the random phase approximation (RPA), as implemented in the CASTEP code[26] with CA-PZ exchange-correlation.[27]

III. RESULTS

In the *h*-BN sheet each B (N) atom is bonded to three N (B) atoms giving rise to repetitive hexagonal planar-layered structure where each B-N bond has a bond length of 1.44 Å. The BNB and NBN bond angles in pure BN sheet are ∼120.0°. The BN unit cell has a lattice parameter of 2.50 Å, which is consistent with the experimental results of Corso *et al.*[28] Our calculations on a single-layer *h*-BN sheet show that it has an indirect band gap of 4.5 eV [Fig. 1(a)], which is in agreement with the LDA result reported by Blasé *et al.*[29] The BE (in eV/atom) of the BN system containing n numbers of B and N atoms (total $2n$ atoms) is calculated using the following formula:

$$\mathrm{BE\,(BN)} = \frac{E_{\mathrm{TOT}}\,(\mathrm{BN}) - n\,[E_{\mathrm{TOT}}\,(\mathrm{B})] - n\,[E_{\mathrm{TOT}}\,(\mathrm{N})]}{2n}.$$

It has a high stability with an estimated BE of ∼7 eV/atom. The phonon DOS and dispersion of *h*-BN sheets are shown in Fig. 3(a). The phonon spectra of *h*-BN sheets cover the frequency range of 0 to ∼1500 cm^{-1}. The B-N bond shows highest phonon DOS at a frequency of 1360 cm^{-1}, which is both IR and Raman active. This is in conformity with the experimental results of Gorbachev *et al.*[30] on monolayer *h*-BN sheet.

IV. FUNCTIONALIZATION OF *h*-BN SHEET

We have studied the effect of chemical modification on the electronic structure of a single-layer *h*-BN sheet by functionalizing it with various atoms/groups of atoms on both sides of the sheet. The mono-atomic groups considered in our study are hydrogen and fluorine, while the other groups can be categorized according to their atomic composition as (a) oxygen-containing groups (viz. OH, CHO, COOH, H_2O), (b) nitrogen-containing groups (viz. CN, NH_2), and (c) hydrocarbon group (viz. CH_3). Out of these groups the *h*-BN sheet does *not* bind H_2O and COOH (carboxyl group) molecules, while it chemisorbs all the other groups mentioned previously with BEs ranging from ∼1.5 to 6 eV, as enlisted

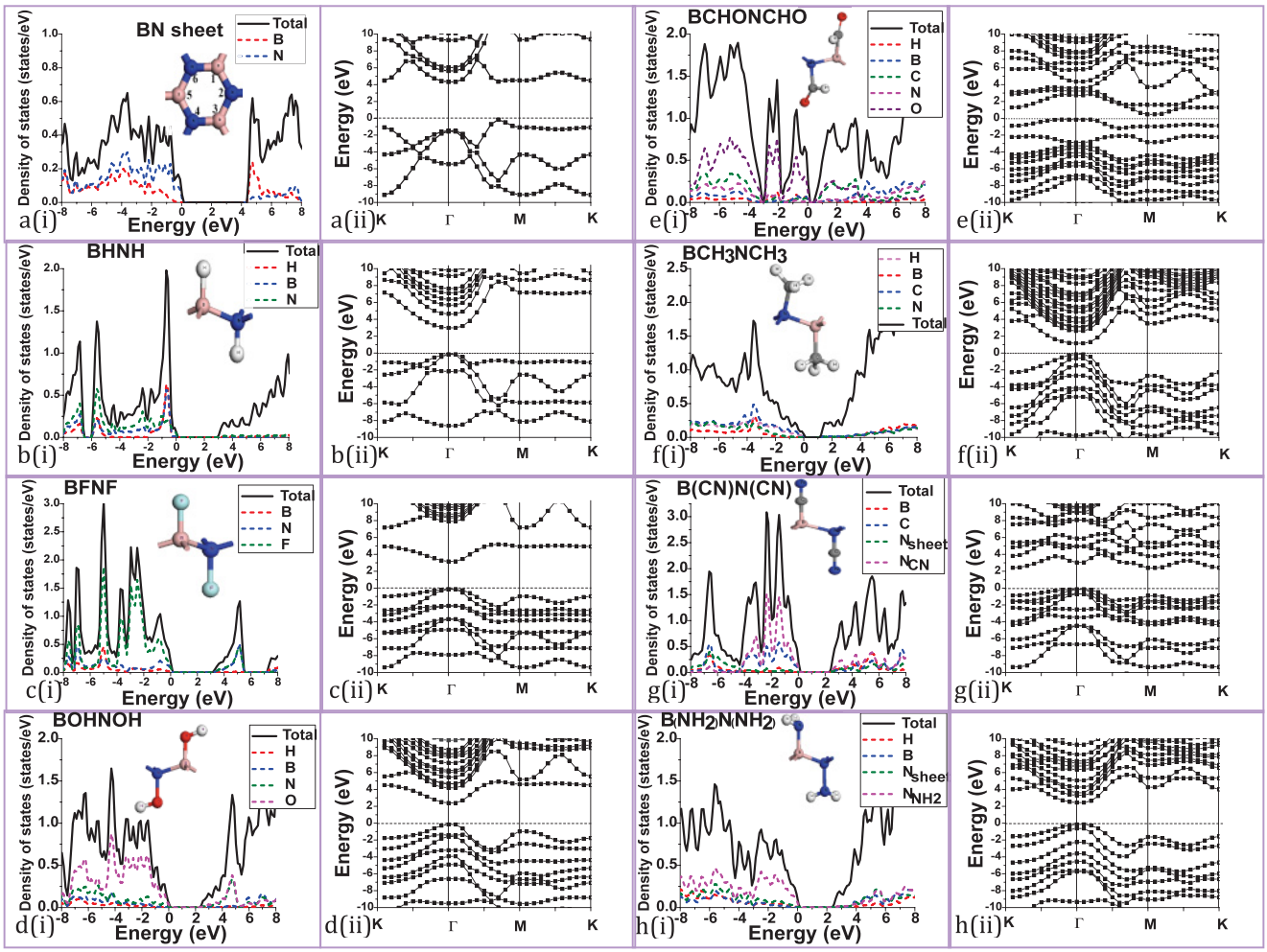

FIG. 1. (Color online) Total/site-projected DOS and band structure of the (a) BN sheet and BN sheet functionalized by (b) H, (c) F, (d) OH, (e) CHO, (f) CH_3, (g) CN, and (h) NH_2.

TABLE I. Band gap, binding energy (BE) of the system, and related properties of the BN sheet functionalized by various groups calculated using LDA. The band gap values have been compared using LDA and GGA.

System	Band gap (eV)		BE of the system (eV/atom)	Chemisorption energy of group bonded to (eV/group)	
	LDA	GGA		B	N
BN	4.5	4.6	7.043	–	–
BHNH	3.0 (direct-Γ)	3.1 (direct-Γ)	4.574	4.30	3.90
BFNF	3.1 (direct-Γ)	3.2 (direct-Γ)	4.850	5.84	3.52
BOHNOH	2.3 (direct-Γ)	2.3 (direct-Γ)	4.663	1.57	2.47
BCNNCN	2.2	2.2	5.746	4.52	3.12
BCH_3NCH_3	1.1 (direct-Γ)	1.2 (direct-Γ)	4.541	2.32	1.82
BNH_2NNH_2	2.5 (direct-Γ)	2.6 (direct-Γ)	4.028	2.58	2.19
BCHONCHO	0.3	0.3	4.9016	2.3	2.1

in Table I. Full functionalization of the sheet takes place in a way that one group gets bonded to each of the B and N atoms, giving rise to various structural conformations, viz. chair, boat, and stirrup, as explained in the Introduction. A hexagonal unit of the *h*-BN sheet is shown in the inset of Fig. 1(a). The B and N atoms in the hexagon are marked from 1 to 6. In the chair conformer the groups chemisorbed at 1, 3, and 5 sites point up the BN plane, while at 2, 4, and 6 sites point down the BN plane. In boat and stirrup conformers the groups pointing up are chemisorbed at 1, 2, 4, and 5, and 1, 2, and 3 sites of the hexagon, respectively, while all of the rest of the sites have groups chemisorbed below the BN plane. We find that other than hydrogenation of the BN sheet (where the stirrup conformation is found to be energetically the most stable conformer by ∼0.2 eV/atom), in all other cases the chair conformation shows highest stability. This is due to the increase in size of the groups (as one goes from H to CH_3), which gives rise to the high repulsive interaction between the groups chemisorbed on consecutive sites in boat and stirrup conformers. In the chair conformer the groups bonded to two consecutive sites face opposite sides of the BN plane (1-up, 1-down geometry), and thus, the distance between two functionalizing groups in any plane is always larger than that in boat and stirrup conformers. Therefore, the repulsive interaction between the chemisorbed groups is lowest in chair conformers (excepting hydrogenation of BN sheet). So, we restrict our calculations to the chair conformation of these chemically modified *h*-BN sheets and discuss their stability and physical properties.

V. STRUCTURE, STABILITY, AND ELECTRONIC PROPERTIES

The stability in terms of BE, electronic band gap, and the chemisorptions energies of the functional groups to the B and N atoms in these chemically modified sheets are enlisted in Table I. The electronic properties and application of hydrogenated *h*-BN sheets have been studied by different groups.[14,31,32] Figure 1(b) shows the structure (of single unit cell), electronic DOS, and band-structure plots of the chair BHNH sheet. A fully hydrogenated *h*-BN sheet (BHNH sheet) is estimated to have BE of ∼4.5 eV/atom. The bond distances and bond angles between various atoms in these functionalized sheets are enlisted in Table II. Functionalization of BN sheets leads to stretching of the B-N bond in all these chemically modified sheets (Table II). In the hydrogenated BN sheet, the B-H and N-H bond lengths are 1.20 Å and 1.03 Å, respectively, which are close to the terminal B-H bond length in B_2H_6 (1.19 Å) and N-H bond length in $N\text{-}H_3$ (1.06 Å), respectively. The HBN (109.5°) and BNH (109.4°) bond angles in BHNH sheet also suggest sp^3 hybridization ($\Phi_{sp}{}^3$). The sheet shows a direct LDA band gap of ∼3.0 eV at the Γ-point. From the site-projected DOS plot, hybridization between the B, N, and H atoms of the sheet can be seen. A fully fluorinated BN sheet (BFNF sheet) is found to have a direct LDA band gap of 3.1 eV at the Γ-point [Fig. 1(c)]. It has stability (BE) of ∼4.85 eV/atom, which is higher than that of its hydrogenated counterpart. The B-F (1.35 Å) and N-F (1.44 Å) bond lengths in the fluorinated BN sheet are larger than the corresponding bond lengths in BF_3 (1.30 Å) and NF_3 (1.37 Å), respectively. The FBN and BNF bond angles in the BFNF sheet are equal (108.3°) in magnitude and also show inclination toward sp^3 hybridization. Functionalization of the BN sheet with alcohol (OH) group also leads to a decrease in the band gap of the sheet. The structure, electronic DOS, and band structure plots of the BOHNOH sheet are shown in Fig. 1(d). It has stability (in terms of BE) of 4.6 eV/atom and also shows a direct LDA band gap of 2.3 eV at the Γ-point. In the BOHNOH sheet the angles subtended by the OH bond to the B and N atoms of the BN sheet [107.3° (∟NBO) and 105.6° (∟BNO), respectively] show significant deviation from $\Phi_{sp}{}^3$. Chemical modification of the *h*-BN sheet with aldehyde (CHO) group is very crucial in this study as it leads to huge lowering in the electronic band gap of the sheet to ∼0.3 eV (LDA). The structural unit, electronic band dispersion, and DOS plots of

TABLE II. Structural (bond lengths and bond angles) and vibrational properties (HVF = highest vibrational frequency mode) of a BN sheet functionalized by various groups (the subscripts in the second column denote the host element to which the dopant atom is bonded). See text for details.

System	Bond	Length (Å)	HVF (cm^{-1})	Bond Angles (deg)	
BN	B-N	1.44	1360	BNB, NBN	119.5, 120.5
	B-H	1.20	2600	HBN	109.5
BHNH	B-N	1.58	830	BNB, NBN	109.5
	N-H	1.03	3245	BNH	109.4
	B-F	1.35	1300	FNB	108.3
BFNF	B-N	1.62	860	BNB, NBN	110.9
	N-F	1.44	1050	NBF	108.3
	O_B-H	0.98	3430	OBN	107.3
BOHNOH	B-O_B	1.40	1240		
	B-N	1.63	850	BNB, NBN	109.8, 110.2
	N-O_N	1.48	1100	BNO	105.7
	O_N-H	0.99	3350		
	C_B-N	1.16	2270	CBN	109.0
BCNNCN	B-C_B	1.52	977		
	B-N	1.73	770	BNB, NBN	109.9
	N-C_N	1.40	1000	BNC	108.9
	C_N-N	1.16	2270		
BCH_3NCH_3	C_B-H	1.06	3390	CBN	110.4
	B-C_B	1.59	1270		
	B-N	1.67	820	BNB, NBN	107.9, 109.4
	N-C_N	1.49	1467		
	C_N-H	1.05	3520	BNC	97.6
BNH_2NNH_2	N_B-H	1.01	3544	NBN	108.3
	B-N_B	1.48	1240		
	B-N	1.74	780	BNB, NBN	109.6, 109.0
	N-N_N	1.49	1300		
	N_N-H	1.01	3386	BNN	108.9
BCHONCHO	C_B-H	1.11	2760		
	C_B-O	1.20	1800		
	B-C_B	1.61	1000	CBN	99.4
	B-N	1.75	720	BNB, NBN	108.7, 109.1
	N-C_N	1.50	1000	BNC	99.8
	C_N-O	1.19	1800		
	C_N-H	1.06	3360		

the BCHONCHO sheet are given in Fig. 1(e). It has the stability (BE) of 4.9 eV/atom. The band structure is mainly modified due to the lowering in unoccupied bands corresponding to C and H atoms near the M-point, which gives rise to an indirect band gap of the sheet. The bond angles subtended by the CHO group to the B and N atoms of the sheet in BCHONCHO sheet are 99.4° (∟CBN) and 99.8° (∟CNB), respectively. Therefore, among all these functionalized sheets, the bond angles in the BCHONCHO sheet show maximum deviation from sp^3 hybridization. Chemical modification of the BN sheet by methyl (CH_3) group alters the electronic band gap of the sheet to an intermediate value as reached by functionalization of the sheet with H, F, OH, and CHO groups. The BCH_3NCH_3 sheet has a BE of ∼4.5 eV/atom and is found to be a direct band gap semiconductor with LDA gap of 1.1 eV at the Γ-point. The corresponding band structure and DOS plots are given in Fig. 1(f). In the occupied region of the DOS, hybridization between the H, B, C, and N atoms of the sheet can be seen. In the BCH_3NCH_3 sheet the CNB bond angle (97.6°) is much lower than $\Phi_{sp}{}^3$, while the NBC bond angle (110.4°) is estimated to be slightly higher than $\Phi_{sp}{}^3$. Chemical functionalization of the sheet with groups containing N, viz. CN and NH_2, decrease the LDA band gap of the corresponding sheets to 2.2 eV (indirect) and 2.5 eV (direct-Γ), respectively. The band structure and DOS plots of BCNNCN and BNH_2NNH_2 sheets are shown in Fig. 1(g) and Fig. 1(h) respectively. While the stability of the BCNNCN sheet (BE of 5.74 eV/atom) is found to be the highest, the stability of the BNH_2NNH_2 sheet (BE of 4.03 eV/atom) turns out to be the lowest among all other chemically modified sheets. In BCNNCN and BNH_2NNH_2 sheets the angles subtended by the chemisorbed group to the B [∟NBC (108.9°) in the BCNNCN sheet and ∟NBN (108.3°) in the BNH_2NNH_2 sheet] and N [∟BNC (108.9°) in the BCNNCN sheet and ∟NNB (108.9°) in the BNH_2NNH_2 sheet] atoms of the sheet also show sp^3 characteristic. The BNB and NBN bond angles

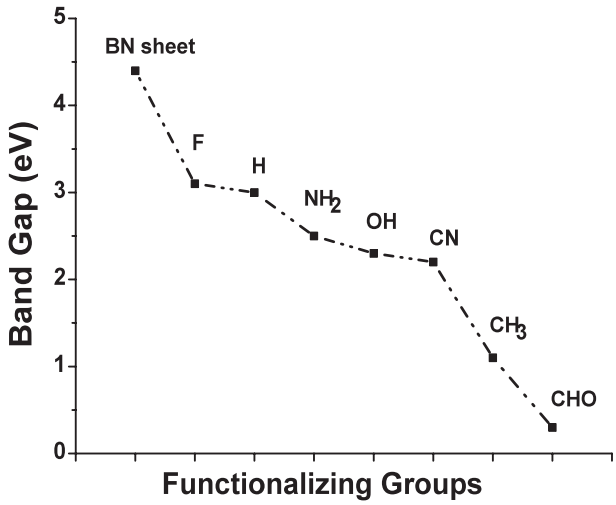

FIG. 2. Summary of band gap variation in the functionalized BN sheet.

in all these functionalized BN sheets are lower than those angles in the pure BN sheet (by ∼9° to 11°), as enlisted in Table II. The band gap manipulation by functionalization of the sheet with different chemical groups is summarized in Fig. 2.

VI. PHONON CALCULATIONS

The phonon dispersion and phonon density plots of the BN sheet functionalized by various groups are shown in Fig. 3. The vibrational modes of various bonds can be predicted from the phonon density plot of these functionalized sheets. The highest vibrational frequencies of various bonds in these functionalized sheets are enlisted in Table II. The phonon spectrum of the hydrogenated BN sheet shows vibrational frequency modes distributed from 0 to ∼3250 cm^{-1}, which indicates the inherent stability of the system [Fig. 3(b)]. The acoustic bands (ranging from 0–600 cm^{-1}) are composed of vibrational modes corresponding to the B-N bonds of the sheet and are distinctly separated from the optical bands (800–3250 cm^{-1}). The phonon dispersion shows two sharp optical bands at 2600 cm^{-1} and 3245 cm^{-1} corresponding to vibrational modes of B-H and N-H bonds, respectively. The highest vibrational frequency modes corresponding to the B-H, B-N, and N-H bonds in the sheet are enlisted in Table II. Though the B atoms are lighter than the N atoms, the highest vibrational frequency mode corresponding to the B-H bond is found to be lower than that of the N-H bond. This is because of the higher chemisorption energy of H (and hence greater bonding) to the B atoms (4.3eV/H) as compared to the N atoms (3.9 eV/H) of the sheet (Table I). The phonon dispersion and DOS of fluorinated BN sheets are shown in Fig. 3(c). All the vibrational frequency modes in the BFNF sheet are found to be real positive, ranging from 0–1500 cm^{-1}. The vibrational modes in the BFNF sheet are much lower in frequency as compared to those in BHNH sheet, which is due to higher mass of the F atoms in the fluorinated sheet. The acoustic and optical bands cannot be clearly separated. However, the last band of optical spectrum is separated from the lower bands and corresponds to vibrational modes corresponding to the B-F bond (1300 cm^{-1}). The highest vibrational mode corresponding to the B-F bond (1300 cm^{-1}) is higher than that of the N-F bond (1050 cm^{-1}), which is due to the lighter mass of B atoms (Table II). The phonon dispersion of the BOHNOH sheet [Fig. 3(d)] shows that the vibrational frequency modes are distributed from 0 to 3400 cm^{-1}. The optical spectra (ranging from 600 to 3400 cm^{-1}) show a number of separated groups of phonons, out of which the highest frequency bands corresponds to the vibration of O_B-H (at 3430 cm^{-1}) and O_N-H bonds (at 3350 cm^{-1}). The chemisorption energy of the OH group (Table I) to the N atoms (2.47 eV/group) is estimated to be higher than that of the same with B atoms (1.57 eV/group), which is in agreement with the highest vibrational frequency corresponding to B-O_B (1240 cm^{-1}) and N-O_N (1100 cm^{-1}) bonds, as enlisted in Table II (O_B and O_N are the symbols used for oxygen bonded to the B and N atoms of the sheet, respectively). The corresponding phonon dispersion and DOS plots of the BCHONCHO sheet are shown in Fig. 3(e). The vibrational modes range from 0 to 3500 cm^{-1}. The optical spectrum (600–3500 cm^{-1}) is composed of many separated single bands of phonon. The highest optical frequency bands at 3350 cm^{-1} and 2750 cm^{-1} correspond to the vibration of the C_N-H and C_B-H bonds. However, the highest vibrational modes of the C_B-O and C_N-O bonds corresponds to a frequency of 1800 cm^{-1}, which gives rise to two overlapping optical bands at this frequency. The highest vibrational frequency corresponding to B-C_B (1000 cm^{-1}) and N-C_N (1000 cm^{-1}) bonds are also found to be close in the BCHONCHO sheet (Table II). This is because even though B is lighter than N, the chemisorption energy (Table I) of the CHO group to B atoms (2.3 eV/group) is higher as compared to that of the N atoms (2.1 eV/group) to the sheet (Table I). The phonon dispersion and phonon DOS plots of the BCH_3NCH_3 sheet are given in Fig. 3(f). The acoustic and optical regions merge with each other in the phonon spectra. In the higher part of optical spectrum, six sharp optical bands can be seen from 3000 cm^{-1} to 3600 cm^{-1}, which correspond to the highest vibrational modes of the C_B-H and C_N-H bonds. The chemisorption energy (Table I) of the CH_3 group to the B atom (2.32 eV/CH_3) is higher than that of the same to the N atom (1.81 eV/CH_3), which also reflects in the highest vibrational frequency corresponding to the B-C_B (1270 cm^{-1}) and N-C_N (1467 cm^{-1}) bonds (Table II). The phonon spectrum of the BCNNCN sheet is shown in Fig. 3(g). All the vibrational frequency modes in the sheet are found to be positive. The phonon spectrum also shows separated groups of phonons. Two sharp optical bands can be seen at a frequency of 2750 cm^{-1}, which corresponds to the highest vibrational modes of both C_B-N and C_N-N bonds. The highest vibrational frequency modes corresponding to the B-C_B (977 cm^{-1}) and N-C_N (1000 cm^{-1}) bonds are close since the chemisorption energy of the CN group to B (4.5 eV/CN) is estimated to be higher than that to N (3.2 eV/CN), as given in Table I. The acoustic and optical bands merge in the vibrational spectrum of the BNH_2NNH_2 sheet, as shown in Fig. 3(h). There are four sharp optical bands at a frequency range of 3000 cm^{-1} to 3600 cm^{-1}, corresponding to the vibrational modes of the N_B-H and N_N-H bonds. The chemisorption energy (Table I) of NH_2 group to B atoms (2.56 eV/NH_2) is found to be higher than that to N atoms (2.19 eV/NH_2) of

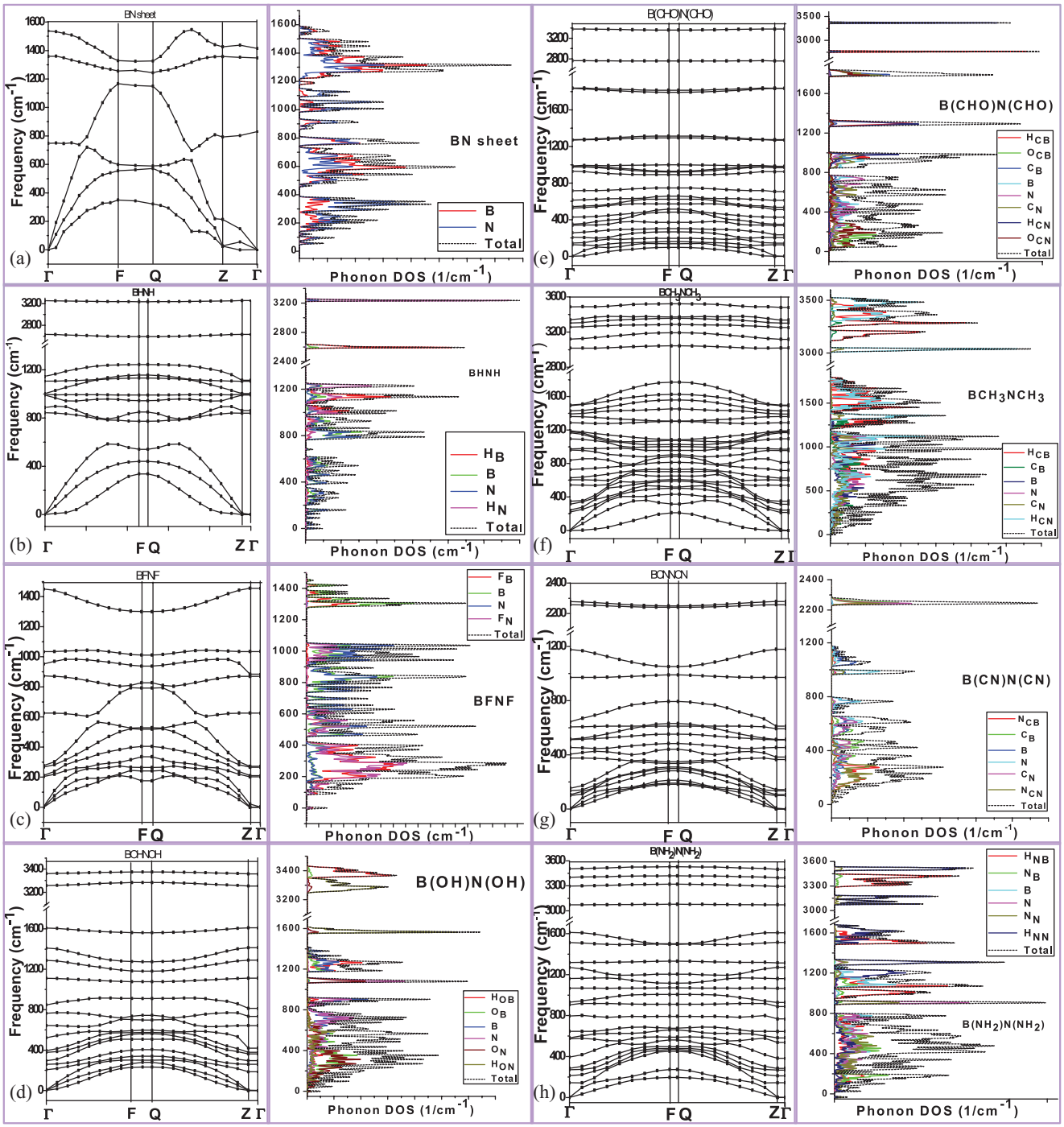

FIG. 3. (Color online) Phonon dispersion and DOS plots of the (a) BN sheet and BN sheet functionalized by (b) H, (c) F, (d) OH, (e) CHO, (f) CH_3, (g) CN, and (h) NH_2.

the sheet, which also reflects in the vibrational frequency of the B-N_B and N-N_N bonds (Table II).

VII. OPTICAL PROPERTIES: ABSORPTION AND CONDUCTIVITY

We have used the DFT approach within the RPA to calculate the optical properties. The real part of the dielectric function has been estimated from the imaginary part of the Kramers-Kronig relationship.[33,34] In order to understand the transition of electrons between the occupied and unoccupied electronic states in these functionalized sheets, we have plotted the optical absorption spectra under light polarized along the Z-axis (i.e., perpendicular to the BN plane). The absorption spectra of a native BN sheet is compared to that of a BN sheet functionalized by H containing passivating groups, viz. H, OH, NH_2, and CH_3 in Fig. 4(a). Our optical absorbtion spectra of a native BN sheet match with the plots of Marinopoulos *et al.*[35] Figure 4(a) shows that pure a h-BN sheet has poor absorption intensity but a high optical band gap of 5.5 eV,[36] as compared to

TABLE III. Mulliken population analysis of the BN sheet and its functionalized derivatives.

System	Atom	Mulliken charge	System	Atom	Mulliken charge
BN	B	0.420	$B(CH_3)N(CH_3)$	H_{CB}	0.150
	N	−0.420		C_B	−0.593
BHNH	H_B	−0.033		B	0.709
	B	0.424		N	−0.633
	N	−0.505		C_N	−0.293
	H_N	0.114		H_{CN}	0.130
BFNF	F_B	−0.243	$B(NH_2)N(NH_2)$	H_{NB}	0.231
	B	0.820		H_{NB}	0.237
	N	−0.383		N_B	−0.622
	F_N	−0.194		B	0.704
B(OH)N(OH)	H_B	0.339		N	−0.562
	O_B	−0.521		N_N	−0.469
	B	0.748		H_{NN}	0.246
	N	−0.469		H_{NN}	0.237
	O_N	−0.437	B(CHO)N(CHO)	H_B	0.082
	H_N	0.340		O_B	−0.165
B(CN)N(CN)	N_B	−0.029		C_B	0.044
	C_B	−0.019		B	0.536
	B	0.608		N	−0.616
	N	–		C_N	0.212
	C_N	0.141		O_N	−0.207
	N_N	−0.055		H_N	0.114

those of its functionalized derivatives. Thus, functionalization of a BN sheet decreases the optical band gap, which is the energy until the absorption is zero. The absorption spectra of the BN sheet functionalized by the previously mentioned passivating groups shows one hump dispersion under polarized light with peak intensity at a single point (i.e., at ∼12.0 eV for

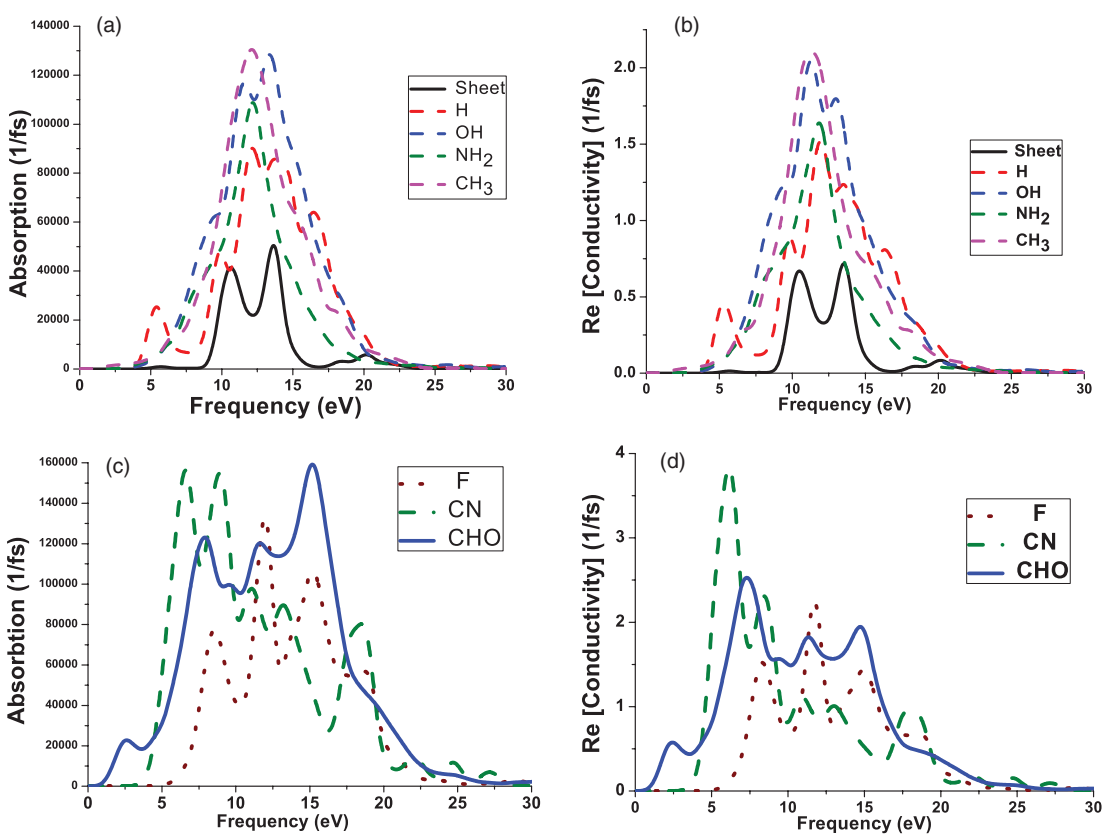

FIG. 4. (Color online) Plots showing the variation of absorption spectrum [(a) and (c)] and real part of conductivity [(b) and (d)] under light polarized along the *c* axis of the BN sheet functionalized by various groups.

H, NH_2, and CH_3 groups, while at ∼13.5 eV for OH group). Thus, the peak intensities of these functionalized sheets are concentrated near the middle portion of the spectrum width. This also reflects in the variation of a real part of conductivity with the energy of incident light. The conductivity in these functionalized sheets reaches their peak value at ∼12.0 eV. On comparing the conductivity peaks with that of a pure BN sheet we find that functionalization increases the conductivity of these sheets. The optical band gap in these functionalized sheets can also be verified from their spectral analysis. The absorption spectra of a BN sheet functionalized by F, CN, and CHO groups [Fig. 4(b)] have multiple peaks, but their peak intensities are higher than that of a BN sheet functionalized by previous passivating groups. The absorption spectra of fluorinated BN sheets show a broad three-hump structure with the middle hump having the highest peak intensity at ∼12.0 eV. The highest peak intensity of the CHO functionalized sheet is shifted to the right (∼16.0 eV) as compared to other spectral lines, but the absorption starts at very low energy (∼0.3 eV), which leads to lowering of the optical band gap. The absorption spectra of a CN functionalized sheet reaches its peak intensity at lower energy (i.e., at 6.5 eV and 8.5 eV) as compared to other sheets. From the conductivity plots we can decipher that a CN functionalized sheet has the highest conductivity occurring at much lower frequency as compared to all other functionalized sheets.

VIII. MULLIKEN POPULATION ANALYSIS

From the Mulliken population analysis[37] of these chemically functionalized sheets and native *h*-BN sheet (see Table II) carried out using the CASTEP programme, the charge state of B and N atoms before and after functionalization can be compared. The native *h*-BN sheet shows a Mulliken charge transfer of +0.42 electrons from B to N atoms of the sheet. However, in most of the functionalized sheets, N gains electrons and acquires a more negative charge state, while B loses electrons to acquire a more positive charge state as compared to their charge state in a native *h*-BN sheet. This is due to the electronegativity difference of the atoms of the sheet and dopant groups. The electronegativity of atoms present in the dopant groups via which the bonding takes place (viz. O in OH; C in CHO; CN, CH_3, and N in NH_2) is lower than their native electronegativity due to transfer of electrons. Therefore, in most of the cases, the electronegativity of the dopant atom via which the bonding with the sheet takes place are found to be higher than B but lower than N atoms of the sheet. Thus, the dopant groups, being more electronegative than B, gain electrons from it, while losing electrons to the N atoms. However, the fluorinated BN sheet is an exception to this generalization. In the BFNF sheet both B and N lose electrons. The reason can be explained from the Pauling electronegativity difference of native B (2.04), N (3.04), and F (3.98) atoms. The electronegativity of F is higher than both B and N atoms, and therefore in the BFNF sheet both B and N loses electrons to F atoms. Thus, in all these functionalized sheets, the dopant atoms undergo charge transfer with the atoms of the sheet, which in turn alter their electronic structure.

The underlying reason for band gap reduction can also be found from the Mulliken population analysis of these sheets. Most of the passivating groups donates electrons to the host atoms of the sheet. As a result of this, the bottom of the conduction band gets lowered due to the increase in the number of unoccupied levels corresponding to the atoms of the chemisorbed groups. However, only in the case of fluorination (where F withdraws electrons from the host atoms of the sheet), the conduction-band bottom arises from the host N-atoms whose number of unoccupied level increases. Therefore, the effective band gap also gets reduced on the fluorination of the sheet.

IX. CONCLUSION

In summary we have performed first principles calculations to estimate the stability and ground-state properties of the *h*-BN sheet chemically functionalized by various groups, viz. H, F, OH, CH_3, CHO, CN, NH_2, etc. Using these dopants, the band gap of these chemically modified sheets can be tuned from 3.2 eV to 0.3 eV. Most of these functional groups, excepting CHO and CN, results in direct band gap semiconductors. Functionalization by the CHO group in particular leads to a sharp decrease in the electronic band gap of the pristine BN sheet to ∼0.3 eV, which is congenial for its usage in transistor-based devices. We have also carried out phonon calculations on these functionalized sheets to show that the frequencies corresponding to all their vibrational modes are real (positive), suggesting their inherent stability. The chemisorption energy of these groups to the B and N atoms of the sheet are found to lie in the range of 1.5–6 eV. The optical absorption and conductivity spectra in these functionalized sheets under light polarized perpendicular to the BN plane show that the optical absorption and conductivity in these functionalized sheets are much higher than that of the native BN sheet.

*msgpd@iacs.res.in

[1] A. K. Geim and K. S. Novoselov, Nat. Mater. **6**, 183 (2007); K. S. Novoselov, A. K. Geim, S. V. Morozov, D. Jiang, Y. Zhang, S. V. Dubonos, I. V. Grigorieva, and A. A. Firsov, Science **306**, 666 (2004).

[2] K. S. Novoselov, A. K. Geim, S. V. Morozov, D. Jiang, M. I. Katsnelson, I. V. Grigorieva, S. V. Dbonos, and A. A. Firsov, Nature (London) **438**, 197 (2005).

[3] C. Lee, X. Wei, J. W. Kysar, and J. Hone, Science **321**, 385 (2008).

[4] K. Nakada, M. Fujita, G. Dresselhaus, and M. S. Dresselhaus, Phys. Rev. B **54**, 17954 (1996).

[5] A. Bhattacharya, S. Bhattacharya, and G. P. Das, Phys. Rev. B **84**, 075454 (2011).

[6] Z. F. Wang, K. Storr, L. Balicas, F. Liu, and P. M. Ajayan, Nat. Mater. **9**, 430 (2010).

[7] D. W. Boukhvalov and M. I. Katnelson, Phys. Rev. B **78**, 085413 (2008).

[8] Marcel H. F. Sluiter and Yoshiyuki Kawazoe, Phys. Rev. B **68**, 085410 (2003).

[9]J. O. Sofo, A. S. Chaudhari, and G. D. Barber, Phys. Rev. B **75**, 153401 (2007).
[10]A. Bhattacharya, S. Bhattacharya, C. Majumder, and G. P. Das, Phys. Rev. B, **83**, 033404 (2011).
[11]D. C. Elias, R. R. Nair, T. M. G. Mohiuddin, S. V. Morozov, P. Blake, M. P. Halsall, A. C. Ferrari, D. W. Boukhvalov, M. I. Katsnelson, A. K. Geim, and K. S. Novoselov, Science **323**, 610 (2009).
[12]M. Topsakal, E. Aktürk, and S. Ciraci, Phys. Rev B **79**, 115442 (2009).
[13]C. G. Lee, Q. Li, W. Kalb, X. Liu, H. Berger, R. W. Carpick, and J. Hone, Science **328**, 76 (2010).
[14]C. Jin, F. Lin, K. Suenaga, and S. Iijima, Phys. Rev. Lett. **102**, 195505 (2009).
[15]A. Bhattacharya, S. Bhattacharya, C. Majumder, and G. P. Das, Phys. Stat. Sol.: Rapid Research Lett. **4**, 368 (2010).
[16]P. Hohenberg and W. Kohn, Phys. Rev. **136**, B864 (1964).
[17]W. Kohn and L. Sham, Phys. Rev. **140**, A1133 (1965).
[18]G. Kresse and J. Hafner, Phys. Rev. B **49**, 14251 (1994); G. Kresse and J. J. Furthmüller, Comput. Mater. Sci. **6**, 15 (1996).
[19]P. E. Blöchl, Phys. Rev. B **50**, 17953 (1994).
[20]D. M. Ceperley and B. J. Alder, Phys. Rev. Lett. **45**, 566 (1980); D. Ceperley, Phys. Rev. B **18**, 3126 (1978).
[21]J. P. Perdew and Y. Wang, Phys. Rev. B **45**, 13244 (1992).
[22]H. J. Monkhorst and J. D. Pack, Phys. Rev. B **13**, 5188 (1976).
[23]W. H. Press, B. P. Flannery, S. A. Tenkolsky, and W. T. Vetterling, *Numerical Recipes* (Cambridge University Press, New York, 1986), Vol. 1.
[24]P. Pulay, Chem. Phys. Lett. **73**, 393 (1980).
[25]K. Refson, S. J. Clark, and P. R. Tulip, Phys. Rev. B **73**, 155114 (2006).
[26]S. J. Clark, M. D. Segall, C. J. Pickard,P. J. Hasnip, M. J. Probert, K. Refson, and M. C. Payne, Zeitschrift fuer Kristallographie. **220**, 567 (2005).
[27]J. P. Perdew and A. Zunger, Phys. Rev. B **23**, 5048 (1981).
[28]M. Corso, W. Auwärter, M. Muntwiler, A. Tamai, T. Greber, and J. Osterwalder, Science **303**, 217 (2004).
[29]X. Blase, A. Rubio, S. G. Louie, and M. L. Cohen, Phys. Rev. B **51**, 6868 (1995).
[30]R. V. Gorbachev, I. Riaz, R. R. Nair, R. Jalil, L. Britnell, B. D. Belle, E. W. Hill, K. S. Novoselov, K. Watanabe, T. Taniguchi, A. K. Geim, and P. Blake, Small **7**, 465 (2011).
[31]J. Zhou, Q. Wang, Q. Sun, and P. Jena, Phys. Rev. B **81**, 085442 (2010).
[32]S. Tang and Z. Cao, Chem. Phys. Lett. **488**, 67 (2010).
[33]R. de. L. Kronig, J. Opt. Soc. Am., **12**, 537 (1926).
[34]H. A. Kramers, Atti. Congr. Intern. Fisici **2**, 545 (1927).
[35]A. G. Marinopoulos, L. Wirtz, A. Marini, V. Olevano, A. Rubio, and L. Reining, Appl. Phys. A **78**, 1157 (2008).
[36]L. Song, L. Ci, H. Lu, P. B. Sorokin, C. Jin, J. Ni, A. G. Kvashnin, D. G. Kvashnin, J. Lou, B. I. Yakobson, and P. M. Ajayan, Nano Lett. **10**, 3209 (2010).
[37]M. D. Segall, R. Shah, C. J. Pickard, and M. C. Payne, Phys. Rev. Lett. **87**, 16317 (1996).